Effects of Slip and Magnetic Fields on the Oscillatory Flow of Jeffrey Fluid in an Elastic Tube

A. SAMATHA, P. MUTHU
Department of Mathematics,
National Institute of Technology,
Warangal,
INDIA

Abstract: - This study investigates the effects of slip conditions and magnetic effects on the oscillatory flow of a Jeffrey fluid within an elastic tube. The perturbation method is employed to derive analytical solutions for the flow characteristics, and Gill's fourth-order method is used to solve the differential equation for the pressure numerically along with the initial conditions. The graphs illustrate how the Womersley, slip velocity, elasticity, Jeffrey, and magnetic parameters affect the mean pressure drop and modulus of wall shear stress. The results reveal that increasing the magnetic field strength and Womersley parameter, the wall shear stress rises in rigid and elastic tubes. Additionally, the slip condition modifies the velocity profile, enhancing fluid motion near the walls. The findings provide insight into the complex interplay of rheology, geometry, and magnetic forces in physiological oscillatory flows.

Key-Words: - Jeffrey fluid, Elasticity, Slip, Magnetic parameter, Oscillatory flow, Perturbation Scheme, Gill's method of fourth order.

Received: September 6, 2025. Revised: March 11 2026. Accepted: May 12, 2026. Published: June 17, 2026.

1 Introduction

The study of oscillatory fluid motion in elastic tubes has wide-ranging applications in biomedical engineering and fluid dynamics. In particular, the Jeffrey fluid model, which accounts for both viscous and elastic properties, is used to represent complex biological fluids such as blood. When blood flows through arteries, it undergoes pulsatile motion influenced by vessel elasticity, viscoelastic nature of the fluid, magnetic effects (such as those encountered in MRI diagnostics and magnetic drug targeting), and wall slip due to micro-scale blood–tissue interactions.

This paper focuses on both the effects of slip velocity and magnetic fields on the oscillatory flow of Jeffrey fluid in an elastic tube. The interaction between the fluids viscoelastic properties, the elasticity of the tube and the external magnetic field, coupled with the impact of slip conditions, is analysed to gain insights into the resultant flow dynamics and wall shear stress variations. Recognizing the features of blood flow via the arteries is also beneficial. It is necessary to comprehend blood flow dynamics to diagnose and treat a variety of Cardiovascular and cerebrovascular diseases. The oscillatory flow of a Jeffrey fluid in an elastic tube with varying cross sections has attracted a lot of attention in the study of fluid mechanics.

Several studies have explored various aspects of Jeffrey fluid flow in elastic or tapered tubes, with or without magnetic effects, [1], [2], [3], [4], [5], [6], [7], [8], [9]. However, most existing works have considered either rigid geometries, neglected slip effects, or evaluated magnetic or viscoelastic influences independently, [10], [11], [12], [13], [14]. Some authors explored various aspects of non-Newtonian or Newtonian fluid flow in elastic or circular tube with suction/injection, [15], [16], [17]. The study of blood flow aims to determine the pressure and flow through the vessels [18], both of which are important to human health. Moreover, although perturbation methods have been widely used for analyzing oscillatory non-Newtonian fluid flows, previous literature has not adequately addressed the convergence criteria of perturbation assumptions in relation to physiological parameter selection, nor has it fully explored the combined impact of slip and magnetic fields in convergent and divergent arterial geometries.

The present work provides a combined analytical and numerical investigation of the viscoelastic effects using the Jeffrey fluid model, slip boundary conditions at the arterial wall, magnetic influence under oscillatory pressure gradient, and elastic deformation of the tube in convergent and divergent geometries. Additionally, this analysis provides a graphical representation of the impact of the elastic, Jeffrey, magnetic, Womersley, and wall velocity (because of slip) parameters on the modulus of wall shear stress and mean pressure drop at the tube wall. No prior study has simultaneously evaluated the coupled effects of slip, magnetic field, and wall elasticity on Jeffrey fluid oscillation in variable cross-sectional geometries, with graphical interpretation of flow behaviour through quantitative assessment of wall shear stress modulus and mean pressure drop.

The present model treats blood as a Jeffrey fluid flowing through a deformable arterial tube with permeability effects. Analytical expressions are derived using the perturbation method, and Gill's fourth-order numerical scheme is used for solving second-order differential equations with coefficients of complex-valued Bessel functions, [19].

Numerical simulations and graphical representations are used to investigate the effects of important dimensionless parameters on wall shear stress and mean pressure drop, such as the Jeffrey parameter, Womersley number, elasticity parameter, magnetic parameter, and slip velocity. The proposed analysis not only offers insight into the complex interaction of these physical factors but also contributes to the enhanced understanding of hemodynamic behavior in elastic arteries under oscillatory conditions.

2 Problem Formulation

We have examined the oscillatory motion of an incompressible Jeffrey fluid in an elastic tube with a circular cross-section and thin walls, taking into account the impact of slip at the tube wall. The elastic tube is assumed to be constrained against longitudinal displacements, as illustrated in Figure 1. The tube radius changes gradually along the axial direction. Here, we considered cylindrical polar coordinates(x, r, Θ).

The constitutive equation for Jeffrey fluid is expressed in Eq. (1), and r = a(x) is expressed in Eq. (2).

$$\bar{T} = -\bar{P}\bar{I} + \bar{s} = \frac{\mu}{1+\lambda_1}(\dot{\gamma} + \overline{\lambda_2}\ddot{\gamma}) \quad (1)$$

$$a(x) = a_0 \, S\left(\frac{\epsilon x}{a_0}\right) \text{ with } S(0) = 1 \quad (2)$$

where $\epsilon = \frac{a_0}{L} \ll 1$

Here, $\bar{T}$, $\bar{s}$ are the Cauchy stress tensor and extra stress tensor. $\overline{P}$ Is the pressure, $\bar{I}$ Is the identity tensor, $\lambda_1$is the ratio of relaxation to retardation times, λ_2 is the retardation time, γ is the shear rate, and dots over the quantities indicate differentiation with respect to time. a_0 is the tube radius is at x = 0, and L represents the characteristic length of the tube (Table 1, Appendix). The fluid in the tube with a uniform radius is represented by the $\epsilon = 0$.

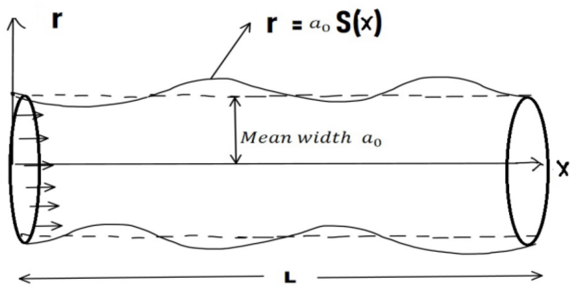

Fig. 1: The Geometry of a Two-Dimensional Elastic Tube
Source: Created by the authors

An axisymmetric fluid flow is governed by the following fundamental equations of motion and continuity:

$$\frac{\partial u}{\partial x} + \frac{\partial v}{\partial r} + \frac{v}{r} = 0 \quad (3)$$

$$\frac{\partial u}{\partial t} + v\frac{\partial u}{\partial r} + u\frac{\partial u}{\partial x} = -\frac{1}{\rho}\frac{\partial p}{\partial x} + \nu\left[\frac{1}{1+\lambda_1}\left(\frac{\partial^2 u}{\partial r^2} + \frac{1}{r}\frac{\partial u}{\partial r}\right) + \frac{\partial^2 u}{\partial x^2}\right] - \frac{\sigma_0 B_0^2 u}{\rho} \quad (4)$$

$$\frac{\partial v}{\partial t} + v\frac{\partial v}{\partial r} + u\frac{\partial v}{\partial x} = -\frac{1}{\rho}\frac{\partial p}{\partial r} + \nu\left[\frac{1}{1+\lambda_1}\left(\frac{\partial^2 v}{\partial r^2} + \frac{1}{r}\frac{\partial v}{\partial r} - \frac{v}{r^2}\right) + \frac{\partial^2 v}{\partial x^2}\right] \quad (5)$$

where, u and v are the axial and radial components of the fluid's velocity. υ is the kinematic viscosity coefficient, ρ is the constant fluid density, p is the pressure, t indicates the time variable, σ_0 is the electrical conductivity of the fluid, B_0 the uniform applied magnetic field, and λ_1 is the Jeffrey parameter.

In the case of longitudinal displacement, we assume that the elastic tube is connected. Due to this, the longitudinal displacement vanishes in the wall's shell equation. The governing equation of radial displacement ξ is expressed as (15):

$$\frac{\partial^2 \xi}{\partial t^2} = \frac{1}{h\rho_0}\left(p - 2\nu\rho\frac{\partial v}{\partial r}\right)_{r=a(x)} - \left(\frac{B}{\rho_0}\frac{\xi}{a^2(x)}\right) \quad (6)$$

where ρ_0 and h indicates the density and thickness of the material of the tube. $B = \frac{E}{1-\sigma^2}$, σ Stands for Poisson's ratio, and E corresponds to Young's modulus, [15].

The equation for the normal component of the fluid velocity at the tube wall is [16]:

$$v - \frac{da}{dx}u = \frac{\partial \xi}{\partial x} \text{ at } r = a(x) \quad (7)$$

The tangential velocity at the wall is non-zero (slip condition), defined as [17]:

$$u + \frac{da}{dx} v = \bar{V}_s \text{ at } r = a(x) \tag{8}$$

Here $\bar{V}_s = V_s e^{i\omega t}$ Represents the oscillatory fluid velocity that causes the slip effect at the boundary, ω denotes the frequency of the oscillation, and $\frac{\partial \xi}{\partial t}$ Is the wall velocity at the tube wall, [17].

The axisymmetry of the flow is

$$\frac{\partial u}{\partial r} = 0 \text{ and } v = 0 \text{ at } r = 0 \tag{9}$$

At the tube's entrance cross section, the flow rate $Q(x)$ is defined as follows:

$$Q = \int_0^{a(x)} 2\pi r u dr = Q_0 e^{i\omega t} \text{ at } x = 0 \tag{10}$$

where Q_0 is constant.

2.1 Analysis

The following dimensionless quantities are introduced for the Eqs. (2), (3), (4), (5), (6), (7), (8), (9), (10).

$$v^* = \frac{v}{\epsilon V_0},\ r^* = \frac{r}{a_0},\ t^* = \omega t,\ q^* = \frac{Q}{Q_0},\ u^* = \frac{u}{V_0},\ V_s^* = \frac{V_s}{V_0},\ x^* = \frac{\epsilon x}{a_0},\ \xi^* = \frac{\xi}{\epsilon a_0},\ p^* = \frac{\epsilon a_0 P}{\rho v V_0},\ (q, q_0) = \frac{(Q, Q_0)}{2\pi a_0^2 V_0},\ M^2 = \frac{\sigma_0}{\mu} B_0^2 a_0^2 \tag{11}$$

Now the Eqs. (2), (3), (4), (5), (6), (7), (8), (9), (10) converted into the dimensionless form by using Eq. (11) and after removing stars are defined as:

$$\frac{\partial u}{\partial x} + \frac{\partial v}{\partial r} + \frac{v}{r} = 0 \tag{12}$$

$$\alpha^2 \frac{\partial u}{\partial t} + \epsilon R\left[v\frac{\partial u}{\partial r} + u\frac{\partial u}{\partial x}\right] = -\frac{\partial p}{\partial x} + \frac{1}{1+\lambda_1}\left[\frac{\partial^2 u}{\partial r^2} + \frac{1}{r}\frac{\partial u}{\partial r}\right] + \epsilon^2 \frac{\partial^2 u}{\partial x^2} - M^2 u \tag{13}$$

$$\epsilon^2\alpha^2 \frac{\partial v}{\partial t} + \epsilon^3 R\left[v\frac{\partial v}{\partial r} + u\frac{\partial v}{\partial x}\right] = -\frac{\partial p}{\partial r} + \epsilon^2\frac{1}{1+\lambda_1}\left[\frac{\partial^2 v}{\partial r^2} + \frac{1}{r}\frac{\partial v}{\partial r} - \frac{v}{r^2}\right] + \epsilon^4 \frac{\partial^2 v}{\partial x^2} \tag{14}$$

$$\epsilon^2 A \frac{\partial^2 \xi}{\partial t^2} = \frac{1}{RS_t^2}\left[p - 2\epsilon^2 \frac{\partial v}{\partial r}\right]_{r=S(x)} - \frac{\xi}{\lambda_2^2 S^2} \tag{15}$$

$$v - u\frac{dS}{dx} = S_t \frac{\partial \xi}{\partial t} \text{ at } r = S(x) \tag{16}$$

$$u + \epsilon^2 \frac{dS}{dx} v = V_s e^{it} \text{ at } r = S(x) \tag{17}$$

$$\frac{\partial u}{\partial r} = 0 \text{ and } v = 0 \text{ at } r = 0 \tag{18}$$

$$q = e^{it} \text{ at } x = 0 \tag{19}$$

where $\alpha^2 = \frac{a_0^2 \omega}{v}, S_t = \frac{\omega a_0}{V_0}, R = \frac{V_0 a_0}{v}, A = \frac{\rho_0 h}{\rho a_0}$ and $\lambda_2^2 = \frac{\rho \omega^2 L^2 a_0}{Bh}$.

Here, α is the Womersley parameter, S_t Is the Strouhal number, R is the Reynolds number, M is the Magnetic parameter, A and λ_2^2 are the dimensionless numbers. λ_2 Denotes the elasticity parameter and $\lambda_2 = 0$ plays the rigid case.

2.1.1 Method of Solution

Examine the flow variable solution by taking the assumption of steady oscillations with the following form:

$$F = e^{it}[F_0 + \epsilon^2 F_2 + O(\epsilon^4)] \tag{20}$$

where $F(x, r, t)$ is used for the flow variables u, v, p and ξ. When Eq. (20) is substituted into Eqs. (12),(13),(14),(15),(16),(17),(18),(19) and the coefficients of the powers of ϵ^0 and ϵ^2 are taken into account, the corresponding equations of zeroth and second order approximations provided with boundary conditions are defined as follows.

ϵ^0 Case:

$$\frac{\partial u_0}{\partial x} + \frac{\partial v_0}{\partial r} + \frac{v_0}{r} = 0 \tag{21}$$

$$\frac{\partial^2 u_0}{\partial r^2} + \frac{1}{r}\frac{\partial u_0}{\partial r} + \delta^2 u_0 = (1+\lambda_1)\frac{\partial p_0}{\partial x} \tag{22}$$

$$\frac{\partial p_0}{\partial r} = 0 \tag{23}$$

$$\xi_0 = \frac{\lambda_2^2 S^2}{\alpha^2 S_t}[p_0]_{r=S(x)} \tag{24}$$

$$v_0 - u_0 \frac{ds}{dx} = iS_t \xi_0 \text{ and } u_0 = V_s \text{ at } r = S(x) \tag{25}$$

$$\frac{\partial u_0}{\partial r} = 0 \text{ and } v_0 = 0 \text{ at } r = 0 \tag{26}$$

$$q_0 = 1 \text{ at } x = 0 \text{ where } \beta^2 = -i\alpha^2, \delta^2 = (1+\lambda_1)(\beta^2 - M^2) \tag{27}$$

ϵ^2 Case:

$$\frac{\partial u_2}{\partial x} + \frac{\partial v_2}{\partial r} + \frac{v_2}{r} = 0 \tag{28}$$

$$\frac{\partial^2 u_2}{\partial r^2} + \frac{1}{r}\frac{\partial u_2}{\partial r} + (1+\lambda_1)\frac{\partial^2 u_0}{\partial x^2} + \delta^2 u_2 = (1+\lambda_1)\frac{\partial p_2}{\partial x} \tag{29}$$

$$\frac{\partial^2 v_0}{\partial r^2} + \frac{1}{r}\frac{\partial v_0}{\partial r} - \frac{v_0}{r^2} + (1+\lambda_1)\beta^2 v_0 = (1+\lambda_1)\frac{\partial p_2}{\partial r} \tag{30}$$

$$\xi_2 = \frac{\lambda_2^2 S^2}{\alpha^2 S_t}\left[p_2 - 2\frac{\partial v_0}{\partial r}\right]_{r=S(x)} + A\lambda_2^2 S^2 \xi_0 \tag{31}$$

$$v_2 - u_2 \frac{dS}{dx} = iS_t \xi_2 \text{ and } u_2 + v_0 \frac{ds}{dx} = 0 \text{ at } r = S(x) \tag{32}$$

$$\frac{\partial u_2}{\partial r} = 0 \text{ and } v_2 = 0 \text{ at } r = 0 \tag{33}$$

$$q_2 = 0 \text{ at } x = 0 \tag{34}$$

By solving the Eqs. (21) - (23) with the boundary conditions Eqs. (24) - (27), we obtain the velocities of zeroth order of u_0 and v_0 are:

$$u_0 = V_s \frac{J_0(\delta r)}{J_0} + \frac{1+\lambda_1}{\delta^2}\frac{dp_0}{dx}\left[1 - \frac{J_0(\delta r)}{J_0}\right] \tag{35}$$

$$v_0 = \frac{1+\lambda_1}{\delta^2}\left[\frac{d^2 p_0}{dx^2}\left(\frac{J_1(\delta r)}{\delta J_0} - \frac{r}{2}\right)\right] + \left[\frac{1+\lambda_1}{\delta^2}\frac{dp_0}{dx} - V_x\right]\frac{J_1}{J_0^2} J_1(\delta r)\frac{dS}{dx} \tag{36}$$

where $J_m(\delta r)$ represents the Bessel function of order m and $J_m \equiv J_m(\delta S)$.

According to Eq. (35), the zeroth-order flux q_0 is as follows:

$$q_0 = \frac{V_s}{J_0}\frac{SJ_1}{\delta} + \frac{(1+\lambda_1)S^2}{2\delta^2}\frac{dp_0}{dx} - \frac{1+\lambda_1}{\delta^3 J_0}\frac{dp_0}{dx} SJ_1 \tag{37}$$

Using the expression Eq. (36) for v_0 and integrating Eq. (30), we get p_2:

$$p_2 = \frac{F(x)}{\delta}(1 - J_0(\delta r)) - \frac{\beta^2 r^2}{4(\beta^2 - M^2)}\frac{d^2 p_0}{dx^2} + G(x) \tag{38}$$

where $F(x)$ from Eq. (38) is:

$$F(x) = \frac{d^2 p_0}{dx^2}\frac{M^2}{\delta J_0(\beta^2 - M^2)} + \left[\frac{1+\lambda_1}{\delta^2}\frac{dp_0}{dx} - V_s\right]\frac{J_1 M^2}{J_0^2}\frac{dS}{dx} \tag{39}$$

where $G(x)$ is unknown. By using the Eqs. (35), (36), and (38) by substituting the corresponding boundary conditions for solving the Eqs. (28) and (29), then we obtain u_2 and v_2 as:

$$u_2 = \frac{1+\lambda_1}{\delta^2}\left[\frac{dG}{dx}\left(1 - \frac{J_0(\delta r)}{J_0}\right)\right] + g_1(x) r J_1(\delta r) + g_2(x) J_0(\delta r) \\ -(1+\lambda_1)\left(\frac{\beta^2 r^2}{4\delta^2(\beta^2 - M^2)} + \frac{(1+\lambda_1)}{\delta^4}\right)\frac{d^3 p_0}{dx^3} \\ + \frac{(1+\lambda_1)F'(x)}{\delta^3} \tag{40}$$

$$v_2 = \frac{-1}{\delta}\left[\frac{dg_1}{dx} r J_2(\delta r) + \frac{dg_2}{dx} J_1(\delta r)\right] + \frac{d^4 p_0}{dx^4}(1+\lambda_1)\left[\frac{\beta^2 r^3}{16\delta^2(\beta^2 - M^2)} + \frac{r(1+\lambda_1)}{2\delta^4}\right] \\ + \frac{1+\lambda_1}{\delta^2}\left[\frac{d^2 G}{dx^2}\left(\frac{J_1(\delta r)}{\delta J_0} - \frac{r}{2}\right) + \frac{dS}{dx}\frac{J_1}{J_0}\frac{dG}{dx} J_1(\delta r)\right] - \frac{(1+\lambda_1)F''(x) r}{2\delta^3} \tag{41}$$

where $g_1(x), g_2(x),\ g_3(x)$ from Eqs. (40), (41) and (43) are:

$$g_1(x) = \frac{(1+\lambda_1)^2}{2\delta^3 J_0}\frac{d^2 p_0}{dx^3} + (1+\lambda_1)^2\frac{dS}{dx}\frac{J_1}{\delta^2 J_0^2}\frac{d^2 p_0}{dx^2} + \frac{(1+\lambda_1)^2}{2\delta^2 J_0^2} g_3(x)\frac{dp_0}{dx} \\ - \frac{(1+\lambda_1)J_1}{2J_0^2}\frac{d^2 S}{dx^2} V_x - \frac{1+\lambda_1}{2}\frac{dS}{dx}\frac{d}{dx}\left(\frac{J_1}{J_0^2}\right) V_x \\ + \frac{dp_1}{dx}\frac{(1+\lambda_1)^2}{2\delta^2}\left[\frac{J_1}{J_0^2}\frac{d^2 S}{dx^2} + \left(\frac{dS}{dx}\right)^2\left(\frac{J_1'}{J_0^2} + \frac{2\delta J_1^2}{J_0^3}\right)\right] \tag{42}$$

$$g_2(x) = \frac{1+\lambda_1}{\delta^2}\frac{d^2 p_0}{dx^2}\left(\frac{\beta^2 S^2}{4J_0(\sigma^2 - M^2)} - \frac{(1+\lambda_1) S J_1}{2\delta J_0^2} + \frac{(1+\lambda_1)}{\delta^2 J_0}\right) \\ + \frac{1+\lambda_1}{\delta^2}\frac{dS}{dx}\frac{d^2 p_0}{dx^2}\left(\frac{S}{2J_0} - \frac{J_1}{\delta J_0^2} - (1+\lambda_1)\frac{S J_1^2}{J_0^2}\right) \\ - \frac{(1+\lambda_1)}{\delta^2}\frac{dp_0}{dx}\left[\left(\frac{dS}{dx}\right)^2\frac{J_1^2}{J_0^2} + \frac{(1+\lambda_1) S J_1}{2J_0^3} g_3(x)\right] \\ + V_s\left[\frac{J_1^2}{J_0^3}\left(\frac{dS}{dx}\right)^2 + \frac{(1+\lambda_1) S J_1^2}{2J_0^3}\frac{d^2 S}{dx^2} + \frac{(1+\lambda_1) S J_1}{2J_0}\frac{dS}{dx}\frac{d}{dx}\left(\frac{J_1}{J_0^2}\right)\right] - \frac{1+\lambda_1}{\delta^3}\frac{F^2(x)}{J_0} \tag{43}$$

$$g_3(x) = J_1\frac{d^2 S}{dx^2} + \left(\frac{dS}{dx}\right)^2 J_1' + \frac{2\delta J_1^2}{J_0}\left(\frac{dS}{dx}\right)^2 \tag{44}$$

Using Eq. (40) for u_2, we obtain the expression for q_2 as,

$$q_2 = \frac{1+\lambda_1}{\delta^2}\left[-\frac{S^2 J_2}{2J_0}\frac{dG}{dx} + \frac{F'(x) S^2}{2\delta}\right] + \frac{S^2 J_2}{\delta} g_1(x) + \frac{S J_1}{\delta} g_2(x) \\ - \frac{1+\lambda_1}{\delta^2}\left(\frac{\beta^2 S^4}{16(\beta^2 - M^2)} + \frac{(1+\lambda_1) S^2}{2\delta^2}\right)\frac{d^3 p_0}{dx^3} \tag{45}$$

Substituting p_2, v_0 and ξ_0 In Eq. (32), we get ξ_2 as:

$$\xi_2 = \frac{\lambda_2^2 S^2}{\alpha^2 S_1}\left[\frac{F(x)}{\delta}(1 - J_0) - \frac{\beta^2 S^2}{4(\beta^2 - M^2)}\frac{d^2 p_0}{dx^2} + G(x) + \frac{1+\lambda_1}{\delta^2}\frac{d^2 p_0}{dx^2} + \frac{2J_1 J_1'}{J_0} V_s\frac{dS}{dx} \\ - \frac{2(1+\lambda_1)}{\delta^2} J_1'\left(\frac{1}{\delta J_0}\frac{d^2 p_0}{dx^2} + \frac{J_1}{J_0^2}\frac{dS}{dx}\frac{dp_0}{dx}\right) + A\lambda_2^2 S^2 p_0\right] \tag{46}$$

Use the conditions (24) and (25), the expressions for v_0 and ξ_0, we obtain the governing equation for pressure:

$$\frac{d^2 p_0}{dx^2} + a(\delta S)\frac{dp_0}{dx} + b(\delta S) p_0 = c(\delta S) \tag{47}$$

where $a(\delta S), b(\delta S), c(\delta S)$ from Eq. (47) are $a(\delta S) = 2\frac{dS}{dx}\frac{J_1^2}{S J_0 J_2}$, $b(\delta S) = -2S\lambda_2^2\frac{J_0}{J_2}\frac{\delta^2}{(1+\lambda_1)\beta^2}$ and $c(\delta S) = 2\delta^2 V_s\frac{(J_1^2 + J_0^2)}{S J_0 J_2 (1+\lambda_1)}\frac{dS}{dx}$.

The initial conditions for p_0 and from Eq. (27), Eq. (37), we can find the condition for $\frac{dp_0}{dx}$ are prescribed as:

$$p_0 = p_{in} = 1 \text{ and } \frac{dp_0}{dx} = -\frac{2\delta}{(1+\lambda_1), J_2}(\delta J_0 - J_1 V_s) \text{ at } x = 0 \tag{48}$$

Using the expressions (41) and (46) for v_2 and ξ_2 along with the condition (32), gives the differential equation $G(x)$ as,

$$\frac{d^2 G}{dx^2} + a(\delta S)\frac{dG}{dx} + b(\delta S) G = d(\delta S) \tag{49}$$

where $d(\delta S)$ from Eq. (49) is:

$$d(\delta S) = 2S\lambda_2^2\frac{\delta^2 J_0}{(1+\lambda_1)\beta^2 J_2}\left[\frac{F(x)}{\delta}(1 - J_0) + \frac{d^2 p_0}{dx^2}\left(\frac{1+\lambda_1}{\delta^2} - \frac{\beta^2 S^2}{4(\beta^2 - M^2)}\right) \\ - \frac{2(1+\lambda_1)}{\delta^2 J_0} J_1'\left(\frac{1}{\delta}\frac{d^2 p_0}{dx^2} + \frac{dS}{dx}\frac{J_1}{J_0}\frac{dp_0}{dx}\right) + \frac{2J_1 J_1}{J_0^2} V_x\frac{dS}{dx} \\ + A\lambda_2^2 S^2 p_0\right] + \frac{2\delta J_0}{(1+\lambda_1)}\left[\frac{dg_1}{dx} + \frac{J_1}{S J_2}\frac{dg_2}{dx}\right] \\ - \left(\frac{\beta^2 S^2 J_0}{8(\beta^2 - M^2) J_2} + \frac{(1+\lambda_1) J_0}{\delta^2 J_2}\right)\frac{d^4 p_0}{dx^4} + \frac{F''(x) J_0}{\delta J_2} \\ + \frac{\delta^2 J_0}{(1+\lambda_1) S J_2}\left(\frac{dS}{dx}\right)^2\left[V_x + i\frac{\lambda_2^2 S^2}{\alpha^2} p_0\right] + \frac{2\delta^2 J_0}{(1+\lambda_1) S J_2}\frac{dS}{dx} \\ \left[S J_1 g_1 + J_0 g_2 - (1+\lambda_1)\left(\frac{1+\lambda_1}{\delta^4} + \frac{\beta^2 S^2}{4\delta^2(\beta^2 - M^2)}\right)\frac{d^2 p_0}{dx^3} + \frac{(1+\lambda_1) F'(x)}{\delta^2}\right] \tag{50}$$

The initial conditions for G and $\frac{dG}{dx}$ are obtained from Eq. (38), Eq. (45) as:

$$G = \frac{\beta^2}{4(\beta^2 - M^2)}\frac{d^2 p_0}{dx^2} - \frac{F(0)}{\delta}(1 - J_0) \text{ and } \frac{dG}{dx} = \frac{2\delta J_0}{(1+\lambda_1)}\left(g_1(x) + \frac{J_1 g_2(x)}{J_2}\right) \\ - \left(\frac{(1+\lambda_1) J_0}{\delta^2 J_2} + \frac{\beta^2 J_0}{8(\beta^2 - M^2) J_2}\right)\frac{d^3 p_0}{dx^3} + \frac{F'(x) J_0}{\delta J_2} \text{ at } x = 0 \tag{51}$$

The Equations Eq. (47) and Eq. (49) were both numerically solved using Gill's method along with the corresponding initial conditions. Then the modulus of p_{mean} is defined as:

$$|p_{mean}| = \{[(p_0 + \epsilon^2 p_2)_{re}]^2 + [(p_0 + \epsilon^2 p_2)_{im}]^2\}^{1/2} \tag{52}$$

The mean pressure drop is defined as:

$$\Delta p = p_{\text{in}} - p_{\text{mean}} \tag{53}$$

The dimensionless wall shear stress T_w Defined in [17] is:

$$T_w = \frac{a_0 T_w}{\mu V_0} \tag{54}$$

$$= e^{it}\left\{\frac{\partial u_0}{\partial r} + \epsilon^2\left[\frac{\partial u_2}{\partial r} - 2\left(\frac{dS}{dx}\right)^2\frac{\partial u_0}{\partial r} + \frac{\partial u_0}{\partial x} - \frac{2}{r}\frac{dS}{dx} v_0 - 4\frac{dS}{dx}\frac{\partial u_0}{\partial x}\right]\right\} + O(\epsilon^4)$$

$$= e^{it}[T_{0w} + \epsilon^2 T_{2w}] + O(\epsilon^4) \tag{55}$$

where T_{0w}, T_{2w} from Eq. (55) are zeroth and second order wall shear stress obtained as:

$$T_{0w} = -\frac{\delta V_s J_1}{J_0} + \frac{(1+\lambda_1)J_1}{\delta J_0}\frac{dp_0}{dx} \quad (56)$$

$$T_{2w} = \frac{4(1+\lambda_1)}{\delta}\left(\frac{dS}{dx}\right)^2 \frac{J_1}{J_0}\frac{dp_0}{dx} - \frac{2}{S}\frac{dS}{dx}\left[V_s\frac{ds}{dx} + i\frac{\lambda_2^2 S^2}{\alpha^2}p_0\right]$$
$$+\frac{1+\lambda_1}{\delta^2}g_4(x) + (1+\lambda_1)J_1\frac{dp_0}{dx}g_5(x) - V_s J_1 g_6(x) + \frac{(1+\lambda_1)J_1}{\delta J_0}\frac{dG}{dx}$$
$$+\delta S J_0 g_1(x) - \delta J_1 g_2(x) - \frac{(1+\lambda_1)\beta^2 S}{2\delta^2(\beta^2 - M^2)}\frac{d^3 p_0}{dx^3} - 2\left(\frac{dS}{dx}\right)^2 \frac{\delta J_1 V_s}{J_0} \quad (57)$$

where $g_4(x), g_5(x), g_6(x)$ from Eq. (57) are:

$$g_4(x) = \frac{SJ_2}{2J_0}\frac{d^3 p_0}{dx^3} + 2\frac{dS}{dx}\frac{J_1^2}{J_0^2}\frac{d^2 p_0}{dx^2} \quad (58)$$

$$g_5(x) = \frac{J_1}{\delta^2 J_0^2}\frac{d^2 S}{dx^2} + \frac{dS}{dx}\frac{1}{\delta^2}\frac{d}{dx}\left(\frac{J_1}{J_0^2}\right) - \frac{2}{\delta J_0}\left(\frac{dS}{dx}\right)^2 \quad (59)$$

$$g_6(x) = \frac{J_1}{J_0^2}\frac{d^2 S}{dx^2} + \frac{dS}{dx}\frac{d}{dx}\left(\frac{J_1}{J_0^2}\right) \quad (60)$$

$$|T_w| = (T_{re}^2 + T_{im}^2)^{\frac{1}{2}} \quad (61)$$

T_{re} and T_{im} are Real and Imaginary part of T_w.

3 Results and Discussion

Gill's method of order 4 [18], is used to numerically evaluate the modulus of wall shear stress $|T_w|$ and the mean pressure drop Δp from Eq. (59), (52) with the corresponding initial conditions. The results are shown in the Appendix in Figure 2, Figure 3, Figure 4, Figure 5, Figure 6, Figure 7 and Figure 8, and Figure 9, Figure 10, Figure 11 and Figure 12, and Figure 13 respectively. By taking ϵ = 0.1, A = 0.055, α = 3, 5, λ_1= 0.0, 0.1, 0.3, 0.5, M = 0, 0.5, 1.0, 1.5 [10], λ_2= 0.0, 0.25, 0.5, and V_s = 0.0, 0.2, 0.4 for the below tube geometries. These approximations are related to the medium-sized arteries.

(i) Convergent tube: S(x) = $e^{-0.1\,x}$

(ii) Divergent tube: S(x) = $e^{0.1\,x}$

3.1 Magnitude of Wall Shear Stress

3.1.1 Convergent Tube

Figure 2 and Figure 3 (Appendix) presents for a different values of M = 0.5, 1, 1.5 with α = 3, 5, λ_1 = 0.1 includes three different cases of slip velocity (V_s= 0, 0.2, 0.4) and elasticity (λ_2= 0, 0.25, 0.5).

For a rigid tube wall, increasing M results in a higher wall shear stress across the axial domain. The effect of M is more pronounced at higher values of x, meaning that in a convergent tube, the influence of the magnetic field strengthens as the flow progresses downstream. The magnitude of wall shear stress is greater than it would be in the case of an elastic tube wall (λ_2 = 0.25). When no slip (V_s = 0), the velocity gradient at the wall is highest and for high slip (V_s = 0.4) reduces the wall shear stress significantly.

Figure 6 and Figure 7 (Appendix) both illustrate the variation of $|T_w|$ along the axial direction in a convergent tube with different values of the Jeffrey parameter (λ_1 = 0, 0.3, 0.5), elasticity (λ_2 = 0, 0.25, 0.5) and slip parameter (V_s = 0, 0.2, 0.4). The difference between the two figures is the influence of the magnitude parameter M = 0, 1.5.

In both figures, $|T_w|$ increases along X, which is expected in a convergent tube where the narrowing cross-section causes a rise in velocity gradients near the wall. However, the rate of increase of $|T_w|$ is higher in Figure 7 (Appendix) (M = 1.5) compared to Figure 6 (Appendix) (M = 0.0), which indicates that the presence of a magnetic field enhances wall shear stress.

The magnetic field dampens velocity fluctuations, leading to a steeper velocity gradient near the wall, which results in higher shear stress.

As increase in λ_1 leads to an increase in $|T_w|$, Jeffrey fluid's viscoelastic effects interact with the magnetic field, amplifying shear stress. As α increase the magnitude of wall shear stress rises.

3.1.2 Divergent Tube

For a divergent tube, $|T_w|$ is plotted in the Figure 4 (Appendix) and in Figure 5 (Appendix) with different values of the Womersley parameter, the magnetic parameter, the slip parameter, the elasticity parameter, and the Jeffrey parameter λ_1 = 0.1.

When M is increased, $|T_w|$ Increases and their overall magnitude decrease in comparison to the convergent case. The modulus of wall shear stress rises in rigid tubes as opposed to elastic tubes, and the effect of slip is less pronounced than in convergent tubes. When there is no slip in a rigid tube, the wall shear stress is the highest across the axial range, and in an elastic tube, the modulus of wall shear stress reduces, and slip significantly reduces shear resistance.

Figure 8 and Figure 9 in Appendix both explain the variation of $|T_w|$ with different values of λ_1 = 0, 0.3, 0.5, λ_2= 0, 0.25, 0.5 and V_s = 0, 0.2, 0.4. The two figures illustrate the difference between the magnitude parameter M = 0, 1.5.

The wall shear stress decreases along x in both cases. Increasing the slip parameter, Jeffrey parameter, and elasticity results in increased shear stress, but they don't alter the overall decreasing trend.

Increasing slip significantly reduces $|T_w|$ with the lowest values observed in Figure 9 (Appendix) and the Jeffrey parameter consistently increases$|T_w|$, regardless of other parameters.

The presence of a magnetic field with M= 1.5 increases shear stress across all cases, but its effect is most pronounced in Figure 9 (where slip is absent) in Appendix. In Figure 9 (Appendix), the slip is highest. The magnetic effect is weaker due to reduced velocity gradients at the wall. As increasing of Magnetic parameter increases, the modulus of wall shear stress increases in both rigid and elastic tubes.

3.2 Mean Pressure Drop

The mean pressure drop is plotted in the Figure 10, Figure 11, Figure 12 and Figure 13 (Appendix) for convergent and divergent tubes. Now the mean pressure drop is plotted versus x (in axial direction). In the Convergent tube, Δp increases along x in all cases compared to the divergent tube. Increasing α = 5 results in significantly larger pressure gradients compared to α = 3.

Increasing slip reduces pressure gradient values, which slightly increases Δp and the magnetic field enhances pressure gradients. Mean pressure drop is higher in all the cases, mainly for M = 1.5 comparing with the other magnetic parameter values. Mean pressure drop values increase continuously with all the magnetic parameter values, and it enhances at each cross-section as it moves from x = 0.0 to 1.0, in tube walls that are both elastic and rigid.

4 Conclusion

This study investigated the effects of slip velocity, magnetic fields, and other parameters on the oscillatory flow of a Jeffrey fluid in an elastic tube. The results demonstrate that an increase in the Womersley parameter enhances the pressure gradients in both geometries. The Jeffrey parameter characterizes the viscoelastic nature of the fluid, and as it increases, the modulus of wall shear stress rises with the effect of the magnetic field. The presence of slip velocity increases the wall shear stress.

By the above analysis, it has been revealed that the rise or fall in the wall shear stress modulus is not only impacted by the parameters α, λ_1, λ_2 and M, but also by the geometry of the tube we are examining. Moreover, observed that the mean pressure drop for tubes with rigid and elastic walls in the magnetic effect enhances with a higher Womersley parameter and falls with a lower Magnetic parameter.

References:

[1] V.K. Sud, G.S. Sekhon and R.K. Mishra, Pumping action on flow by a magnetic field, Bulletin Mathematical Biology, Vol.39, 1977, pp. 385-390. https://doi.org/10.1007/bf02462917.

[2] B. Jyothi and B. Satyanarayana, Effects of Magnetic field on the flow of a Jeffrey fluid through a porous medium in an annulus with peristalsis, Journal of Mathematical and Computational Science, series.5, No.2, 2015, pp. 207-221. ISSN: 1927-5307.

[3] C. H. Badari Narayana, S. Sreenadh and P. Devaki, Oscillatory flow of a Jeffrey fluid in an elastic tube of variable cross-section, Advances in Applied Science Research, series.3, No.2, 2012, pp. 671-677: ISSN: 0976-8610.

[4] A. Kavitha, R.H. Reddy, A.N.S. Srinivas, S. Sreenadh and R. Saravana, Peristaltic pumping of a Jeffrey fluid between porous walls with suction and injection, International Journal of Mechanical and Materials Engineering, Vol.7, No.2, 2012, pp. 152-157.

[5] S. Sreenadh, P. Devaki, Diwakar Reddy and Krishnaiah, Unsteady flow of a Jeffrey fluid in an elastic tube with a stenosis, International Conference on Fluid Dynamics and Thermodynamics Technologies, Vol.33, 2012: https://studylib.net...: Accessed 18 Aug. 2023

[6] A. Aamir, S. Asghar, Analytical solution for Oscillatory flow in a Channel for Jeffrey fluid, American Society of Civil Engineers, series.27, 2014, pp. 644-651: https://doi.org/10.1061/(ASCE)AS.1943-5525.0000298.

[7] N. Santhosh, G. Radhakrishnamacharya, Jeffrey fluid flow through a narrow tubes in the presence of a Magnetic field, Procedia Engineering, 127, 2015, pp. 185-192. https://doi.org/10.1016/j.proeng.2015.11.325.

[8] S. Sreenadh, K. Komala, A.N.S. Srinivas, Peristaltic pumping of a power – Law fluid in contact with a Jeffrey fluid in an inclined channel with permeable walls, Ain Shams Engineering Journal, Vol.8, Issue.4, 2017, pp. 605-611. https://doi.org/10.1016/j.asej.2015.08.019.

[9] G. Manjunatha and C. Rajashekhar, Slip Effects on Peristaltic Transport of Casson Fluid in an Inclined Elastic Tube with Porous Walls, Journal of Advanced Research in Fluid Mechanics and Thermal Sciences, Series.43, Issue.1, 2018, pp. 67-80: ISSN: 2289-7879.

[10] C.K. Selvi and A.N.S. Srinivas, Pulsatile flow of Jeffrey fluid in a porous elastic tube with variable cross - section under the effect of magnetic field, Thermal Science and Engineering Progress, Vol.8, 2018, pp. 439-447. https://doi.org/10.1016/j.tsep.2018.08.019.

[11] R. Padma, R. Tamil Selvi, and R. Ponalagusamy, Effects of slip and magnetic

field on the pulsatile flow of a Jeffrey fluid with magnetic nanoparticles in a stenosed artery, The European Physical Journal - Plus, 2019, pp. 134-221. https://doi:10.1140/epjp/i2019-12538-9

[12] B. Sana, U. Saif, I. Khan and Md. Fayz-Al-Asad, Transient Flow of Jeffrey Fluid over a Permeable Wall, Hindawi Mathematical Problems in Engineering, 2019, pp. 1-9. https://doi.org/10.1155/2021/9999949.

[13] K. Chakradhar, K. Nandagopal, G. Bhagyalaxmi and V. Prashanthi, Peristaltic Transport Of Casson Fluid In A Vertical Permeable Channel With Suction And Injection By Numerical Technique, Journal of Pharmaceutical Negative Results, Vol.13, Issue.8, 2022, pp. 402-411. https://doi.org/10.47750/pnr.2022.13.S08.054.

[14] B. Sana, U. Saif, S. Amnah Al-Johani, I. Khan and A. Mulugeta, Effects of MHD and Porosity on Jeffrey Fluid Flow with Wall Transpiration, Hindawi Mathematical Problems in Engineering, 2022, pp. 1-9. https://doi.org/10.1155/2022/6063143.

[15] A. Ramachandra Rao, Oscillatory flow in an elastic tube of variable cross-section, Acta Mechanica, Vol.46, 1983, pp. 155-165. https://doi.org/10.1007/BF01176771.

[16] P. Chandra and J. K. Prasad, Pulsatile flow in circular tubes of varying cross-section with suction/injection, Journal of Austral. Math. Soc. Sen. B, Vol.35, No.3, 1994, pp. 366-381.

[17] C. K. Selvi and A. N. S. Srinivas, Oscillatory flow of a Casson fluid in an elastic tube with variable cross section, Applied Mathematics and Nonlinear Sciences, Vol.3, No.2, 2018, pp. 571-582. https://doi.org/10.2478/AMNS.2018.2.00044.

[18] Y. C. Fung, Biomechanics-II: Circulation, Springer Science and Business Media, 1997. http://dx.doi.org/10.1007/978-1-4757-2696-1.

[19] M. Abramowitz, Handbook of mathematical functions, National Bureau of Standards, 1964. ISSN: 0025-5718.

Contribution of Individual Authors to the Creation of a Scientific Article (Ghostwriting Policy)

The authors equally contributed in the present research, at all stages from the formulation of the problem to the final findings and solution.

Sources of Funding for Research Presented in a Scientific Article or Scientific Article Itself

No funding was received for conducting this study.

Conflict of Interest

The authors have no conflicts of interest to declare that are relevant to the content of this article.

APPENDIX

Table 1. Nomenclature

$\bar{T}$	Cauchy stress tensor	B_0	Uniform applied magnetic field
$\bar{s}$	Extra stress tensor	ξ	Radial displacement
$\bar{P}$	Pressure	σ	Poisson's ratio
$\bar{I}$	Identity tensor	**E**	Young's modulus
λ_1	Jeffrey Parameter (ratio of relaxation to retardation time)	ρ_0, h	Density, thickness of the material of the tube
λ_2	Retardation time	V_s	Slip Velocity
γ	Shear rate	ω	Frequency of oscillation
.	Differentiation w. r. t time	λ_2	Elasticity parameter
a_0	Tube radius	α	Womersley parameter
L	Characteristic length of the tube	S_t	Strouhal number
u	Axial velocity	**R**	Reynolds number
v	Radial velocity	**M**	Magnetic parameter
υ	Kinematic viscosity coefficient	ϵ	Variation parameter
ρ	Constant fluid density	T_w	Wall shear stress
t	Time variable	Δp	Pressure drop
σ_0	Electrical conductivity of the fluid	$J_m(\delta r)$	Bessel function of order m

Source: Created by the authors

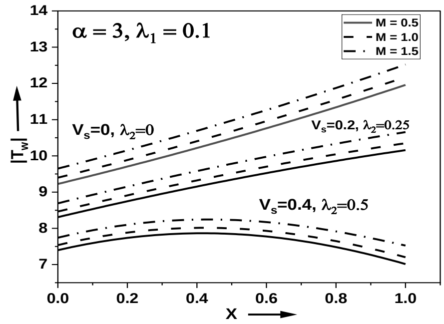

Fig. 2: $|T_w|$Versus x for a convergent tube with $\alpha = 3$, $\lambda_1 = 0.1$ Source: Created by the authors.

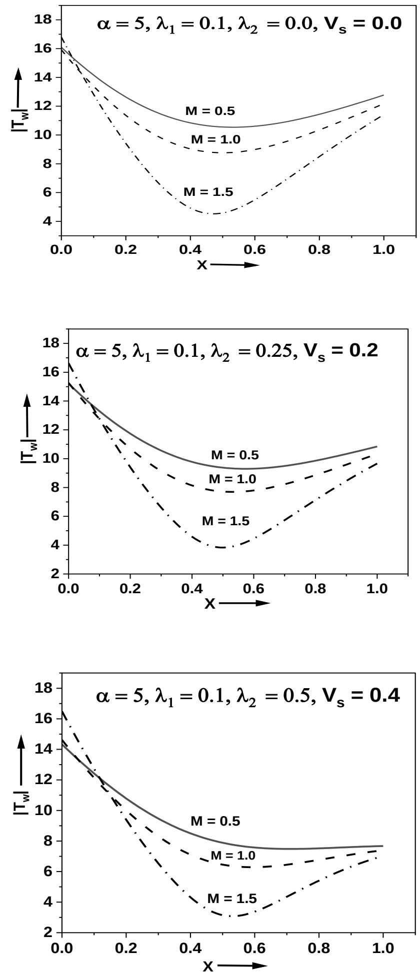

Fig. 3: $|T_w|$ Versus x for a convergent tube with $\alpha = 5$, λ_1=0.1 Source: Created by the authors.

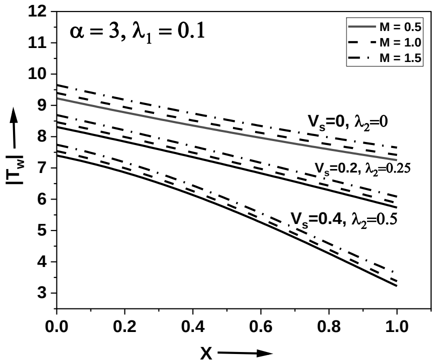

Fig. 4: $|T_w|$ Versus x for a divergent tube with $\alpha = 3$, $\lambda_1 = 0.1$ Source: Created by the authors.

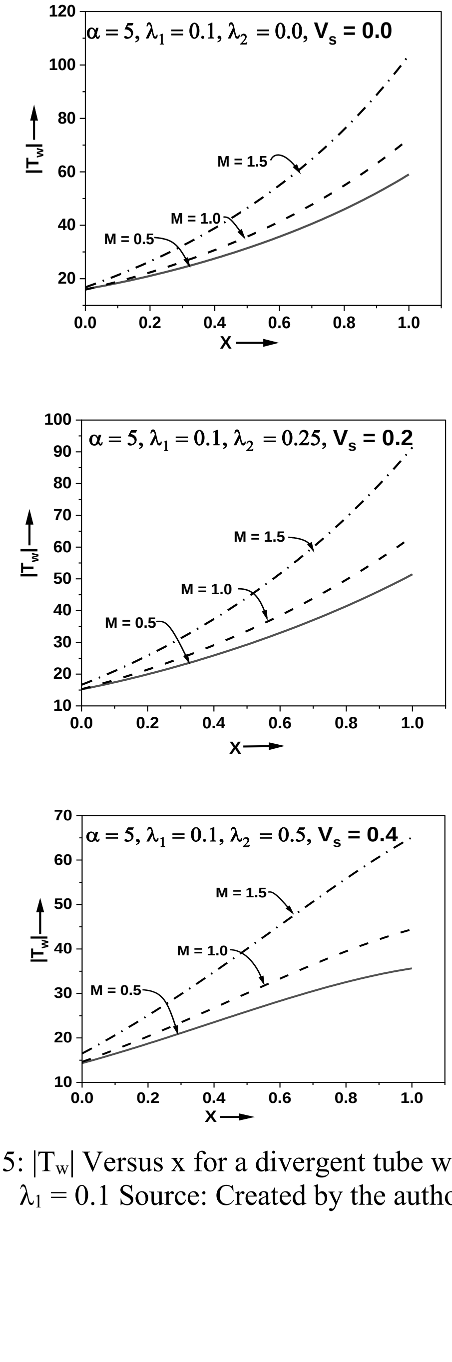

Fig. 5: $|T_w|$ Versus x for a divergent tube with $\alpha = 5$, $\lambda_1 = 0.1$ Source: Created by the authors.

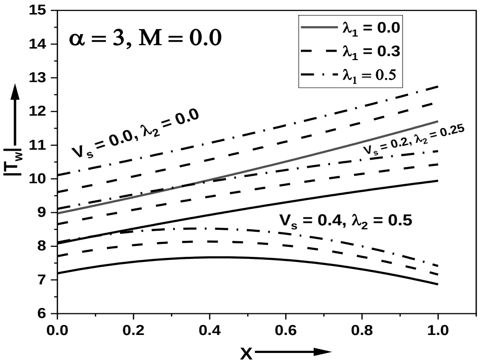

Fig. 6: $|T_w|$ Versus x for a convergent tube with $\alpha = 3$, $M = 0$ Source: Created by the authors.

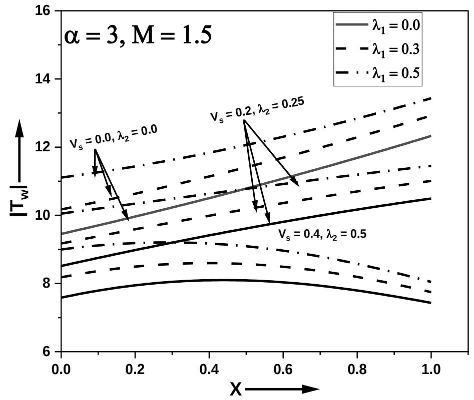

Fig. 7: $|T_w|$ Versus x for a convergent tube with $\alpha = 3$, $M = 1.5$ Source: Created by the authors.

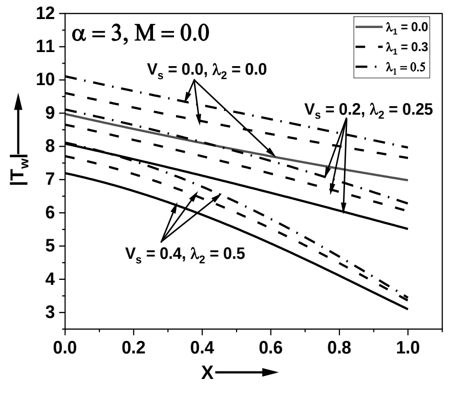

Fig. 8: $|T_w|$ Versus x for a divergent tube with $\alpha = 3$, $M = 0$ Source: Created by the authors.

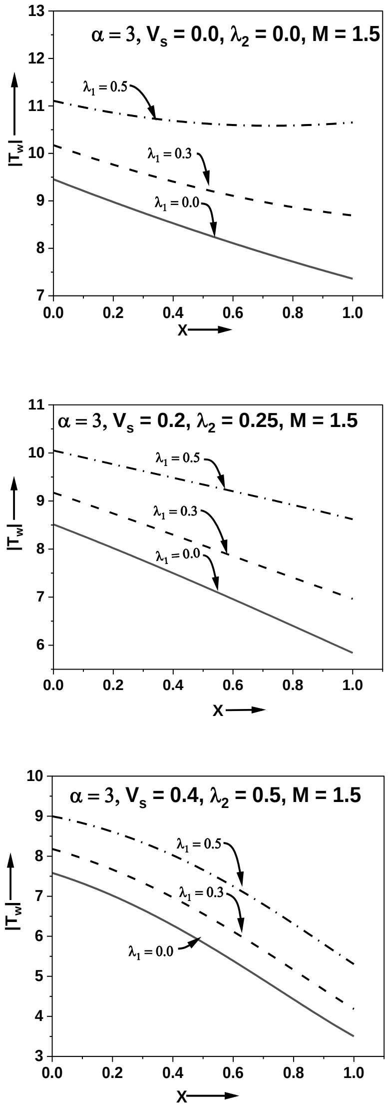

Fig. 9: $|T_w|$ Versus x for a divergent tube with $\alpha = 3$, $M = 1.5$ Source: Created by the authors.

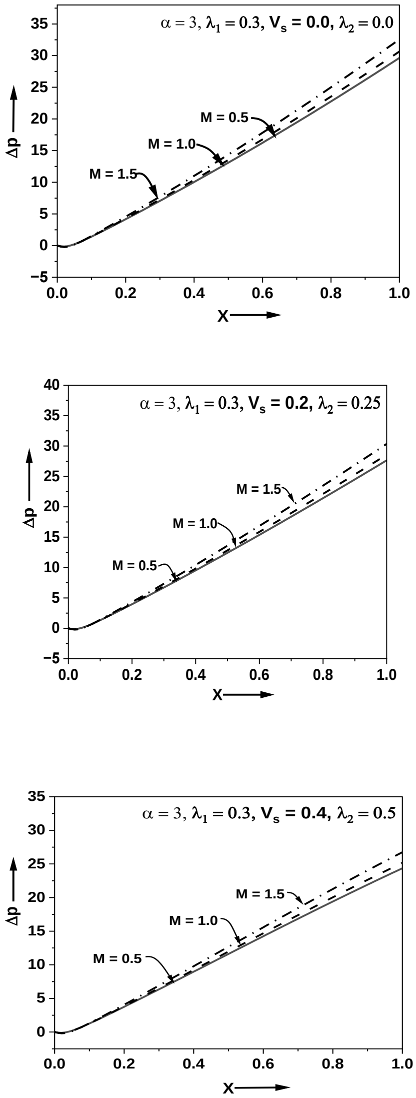

Fig. 10: Δp Versus x for a convergent tube with $\alpha = 3$, $\lambda_1 = 0.3$ Source: Created by the authors.

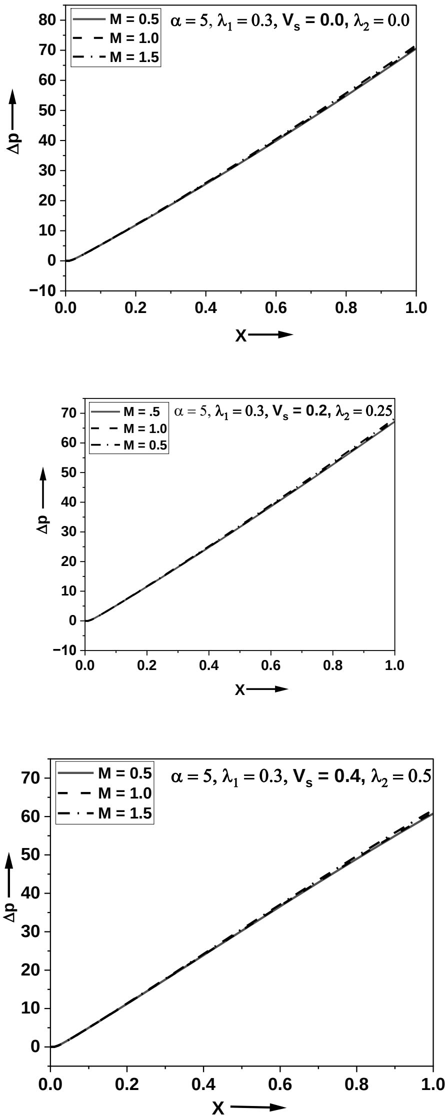

Fig. 11: Δp Versus x for a convergent tube with $\alpha = 5$, $\lambda_1 = 0.3$ Source: Created by the authors.

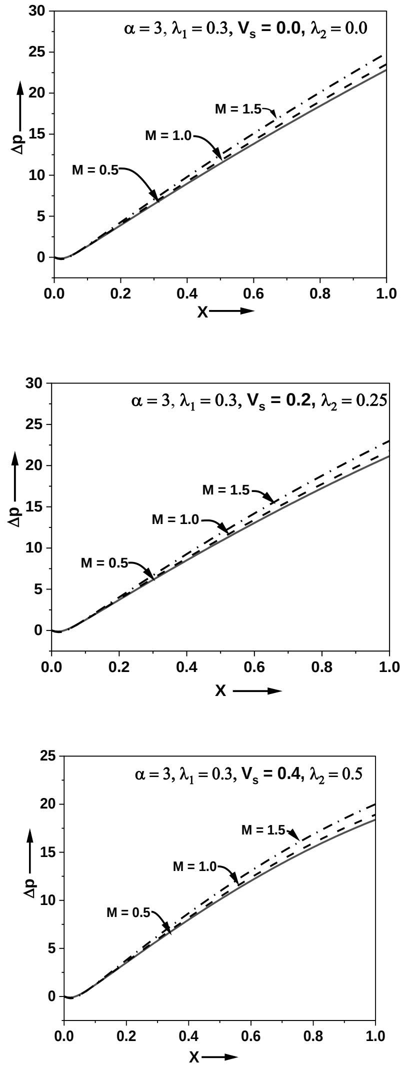

Fig. 12: Δp Versus x for a divergent tube with $\alpha = 3$, $\lambda_1 = 0.3$ Source: Created by the authors.

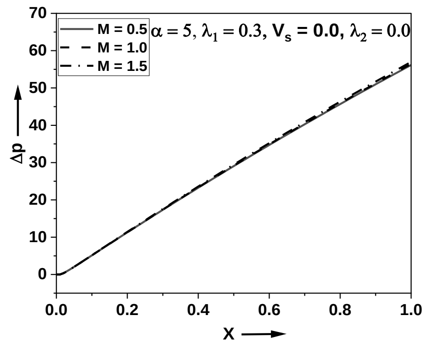

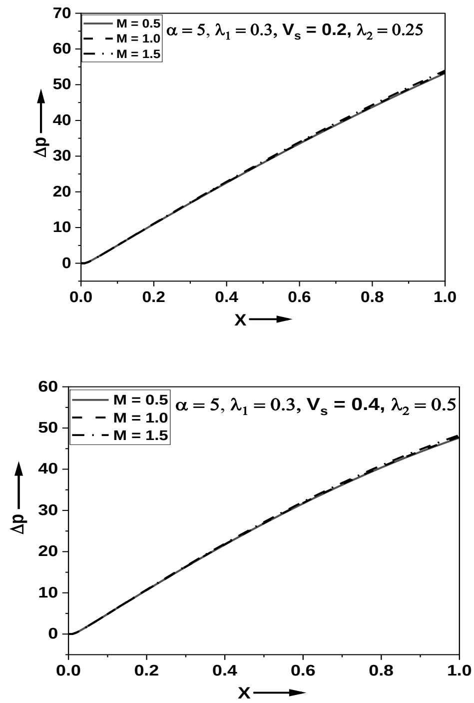

Fig. 13: Δp Versus x for a divergent tube with $\alpha = 5$, $\lambda_1 = 0.3$ Source: Created by the authors.